



Chrysanthos Farmakis, Panayiotis Dimitriadis, Vasilis Bellos, Panos Papanicolaou and Demetris Koutsoyiannis
Department of Water Resources and Environmental Engineering, School of Civil Engineering, National Technical University of Athens

1 Introduction

The last few years that followed the entry into force of the EU Directive 2007/60 on the assessment and management of flood risk, the need for establishing flood risk and flood hazard maps in order to quantify the potential consequences of a flood event to the human factor, the environment, the local economy etc. The establishment of the maps should be followed by measures to manage floods and minimize the possible damages and human losses.

On several occasions, hydrodynamic models are applied in order to establish flood risk and flood hazard maps and evaluate the impacts of floods. More often these models are treated as deterministic tools and, as a result, the uncertainties stemmed from the modelling simplifications and assumptions are ignored (Koutsoyiannis et al. 2012, Dimitriadis et al. 2017). Specifically, when the spatial propagation of a flood wave is of interest the highest uncertainties emerge at the boundary conditions, at the model input parameters and even at the model structure. (Papaioannou et al. 2016, Bellos et al. 2017, Domeneghetti et al. 2013)

2 Aim of this research

The aim of this research is to examine the aforementioned sources of uncertainty in benchmark scenarios. The models tested are HEC-RAS (for steady and unsteady hydraulic conditions), the quasi-two-dimensional LISFLOOD-FP (for steady and unsteady hydraulic conditions), FLO-2D (with two different configurations of the channel geometry), a two-dimensional scheme of the OpenFOAM (on steady hydraulic conditions) and simple model using the Manning equation for open channel flow on steady state conditions. In each model a sensitivity analysis is performed by varying the grid resolution, the input discharge, the roughness coefficient in the channel and floodplain, and the channel longitudinal and lateral gradient (Dimitriadis et al. 2016). After statistically analyzing the fluctuation of the output parameters (the inlet and the outlet water depth and the water volume), the uncertainty in the different model configurations is quantified and compared.

8 Box plots of the water depth of the channels' upstream and downstream cell/section and box plots of the flood volume

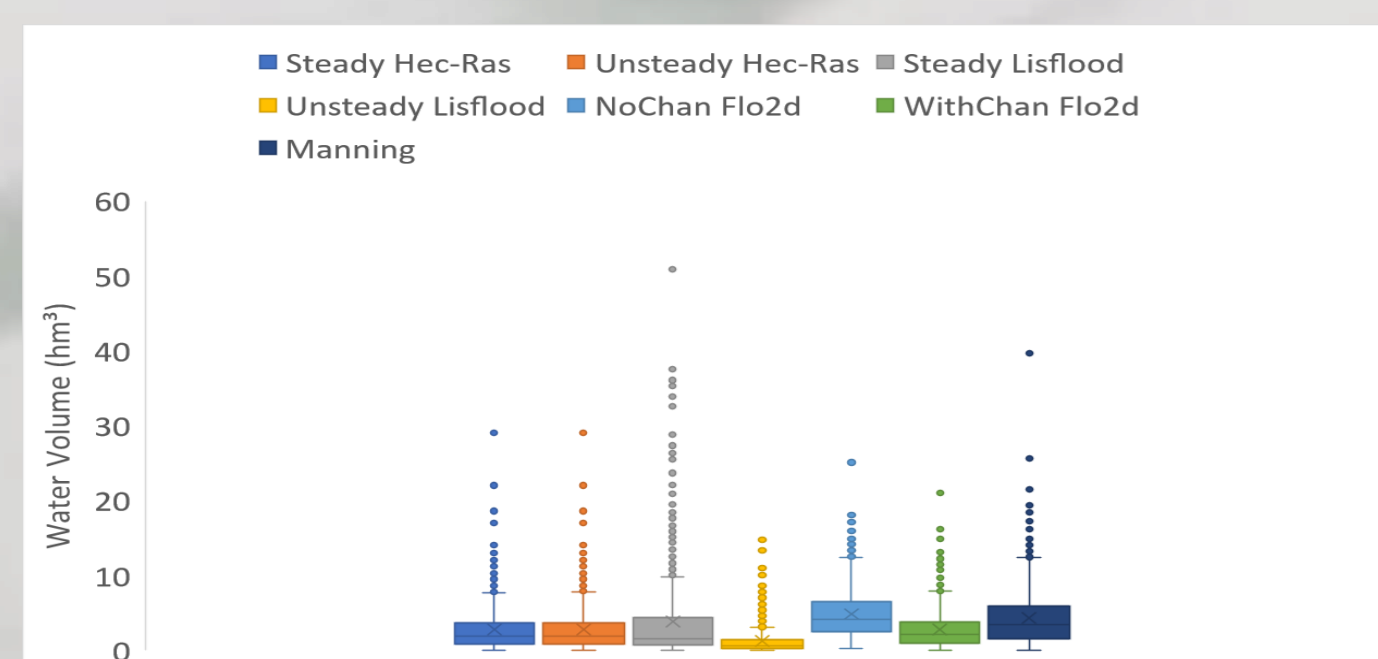


Figure 7: Box plots of the flood volume

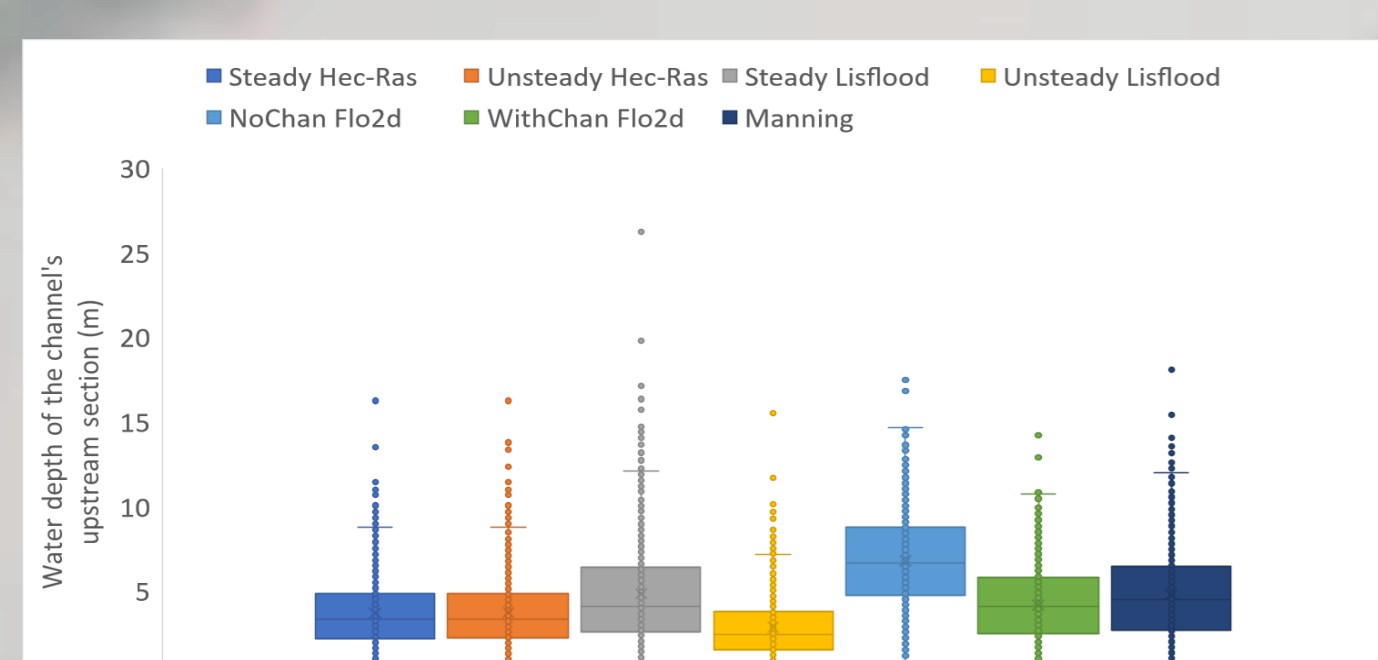


Figure 8: Box plots of the water depth of the channels' upstream cell/section

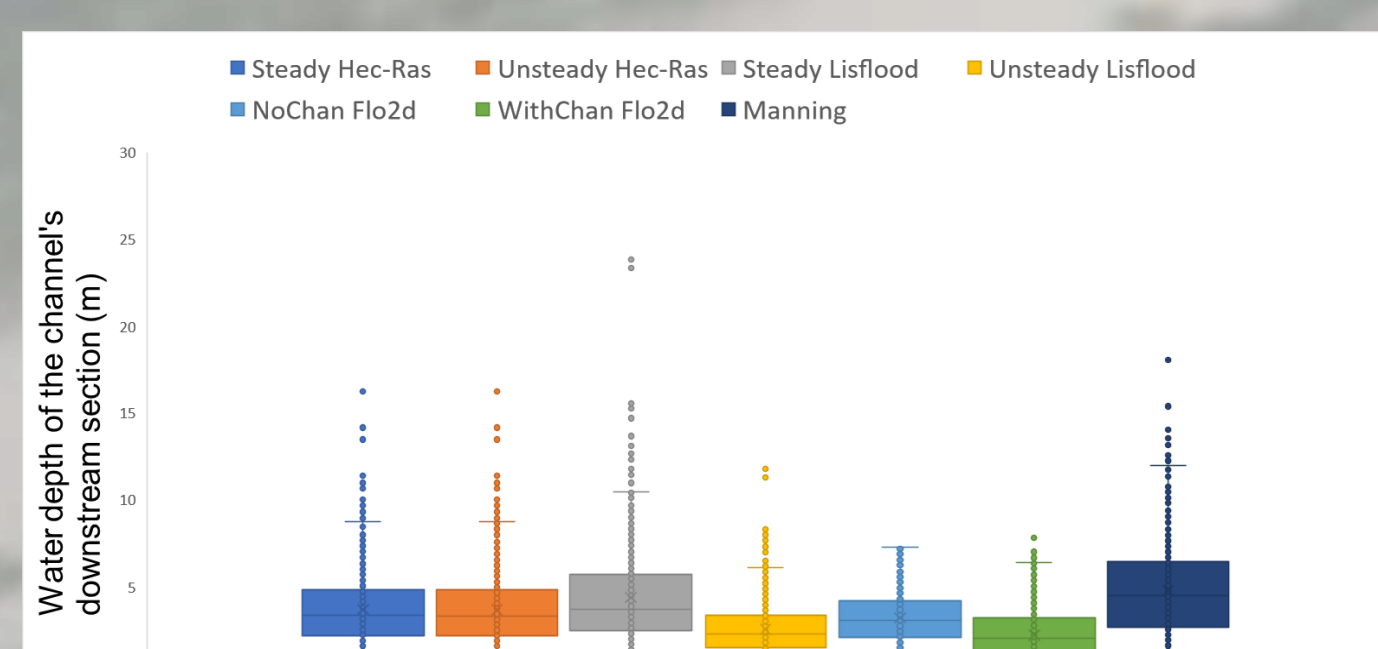


Figure 9: Box plots of the water depth of the channels' downstream cell/section

3 Model setup and input data

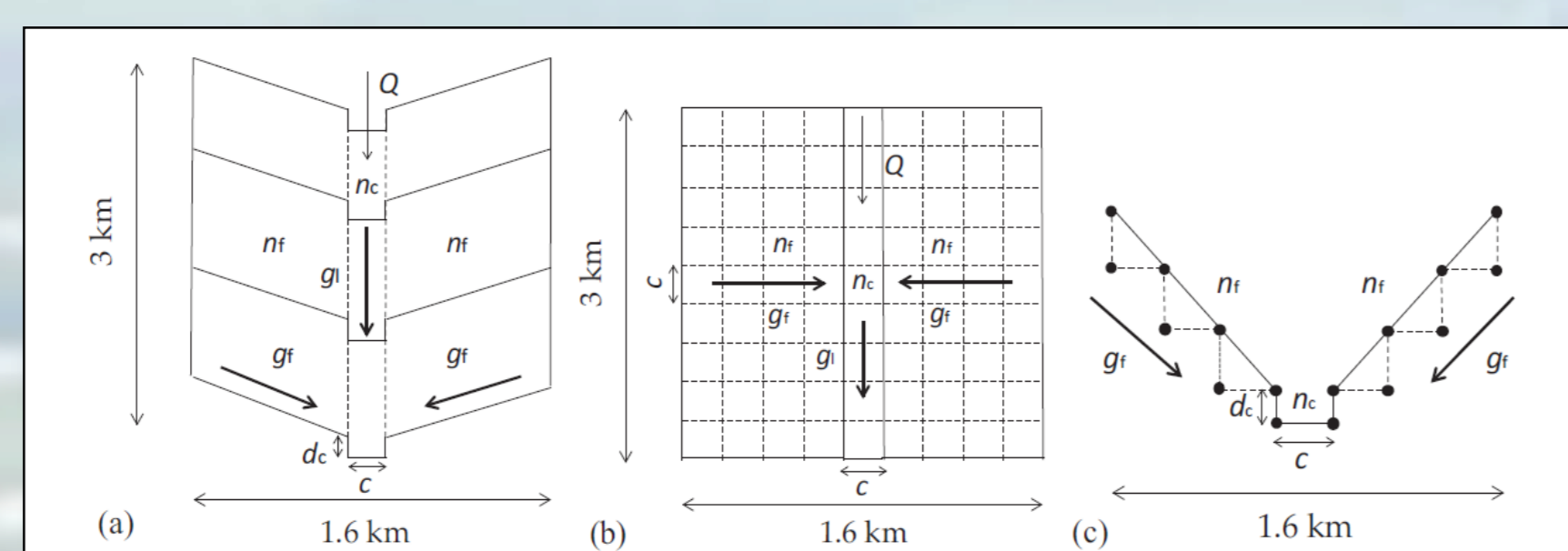


Figure 1: Layout of benchmark tests and associated input variables: (a) perspective view, (b) plan view, and (c) cross sectional view, where solid lines represent the continuous geometry, implemented within HEC-RAS, while dashed lines represent the raster-based geometry, implemented within LISFLOOD-FP and FLO-2D

Variable	Symbol and units	Min	Max
Upstream flow	Q (m ³ /s)	100	5000
Longitudinal gradient	g _l (%)	0.1	5
Lateral gradient	g _r (%)	0.1	5
Roughness coefficients (channel)	n _c	0.01	0.1
Roughness coefficients (floodplain)	n _f	0.05	0.3
Model resolution (channel width)	c (m)	50	100

Table 1: Variables used within sensitivity analysis and associated range of feasible values; all variables are uniformly distributed, except for the model resolution determined by the channel width, which takes three discrete values with equal probability (50 or 100 m).

9 Q-Q plots of the water depth of the channels' upstream and downstream cell/section and Q-Q plots of the flood volume

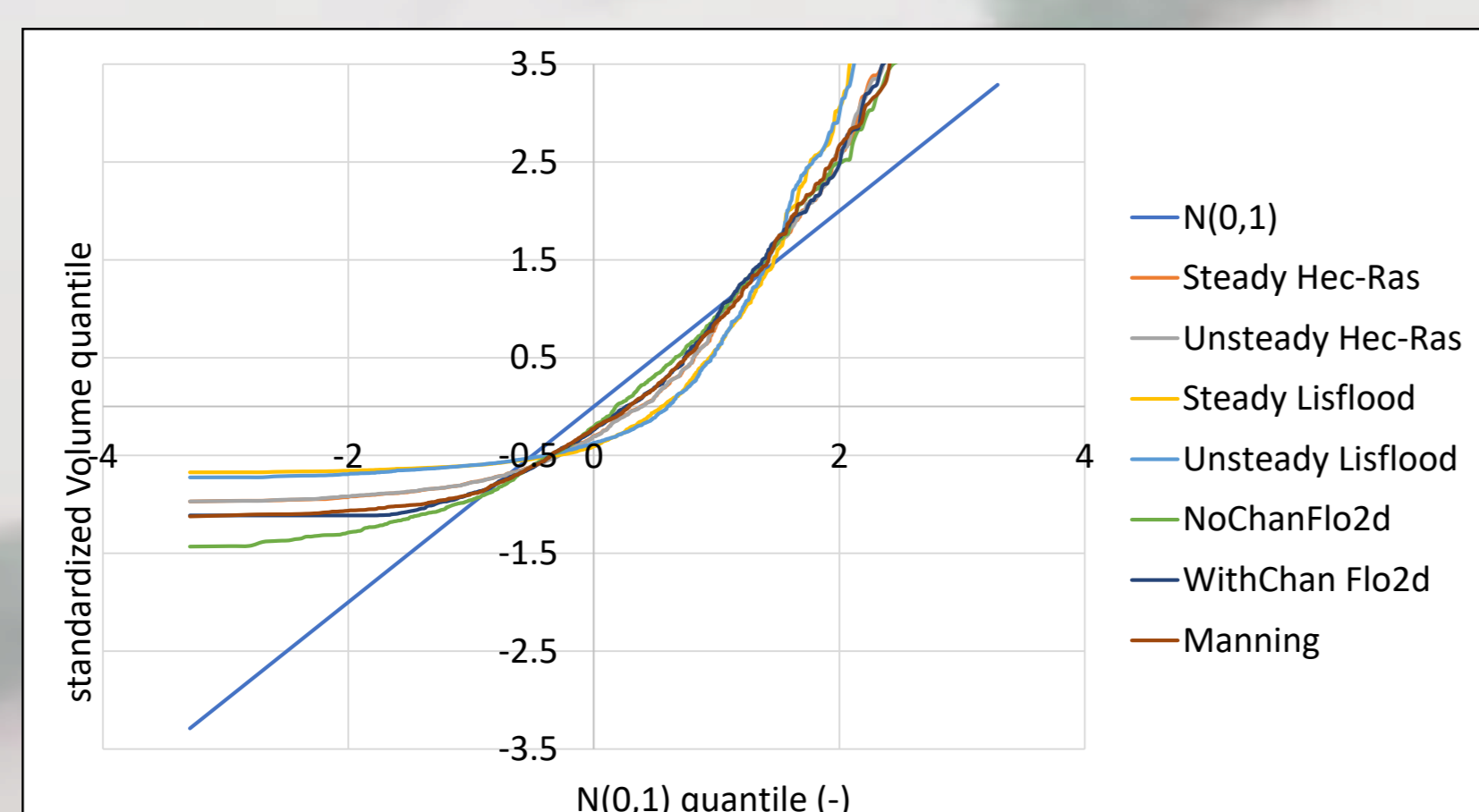


Figure 10: Q-Q plots of the flood volume

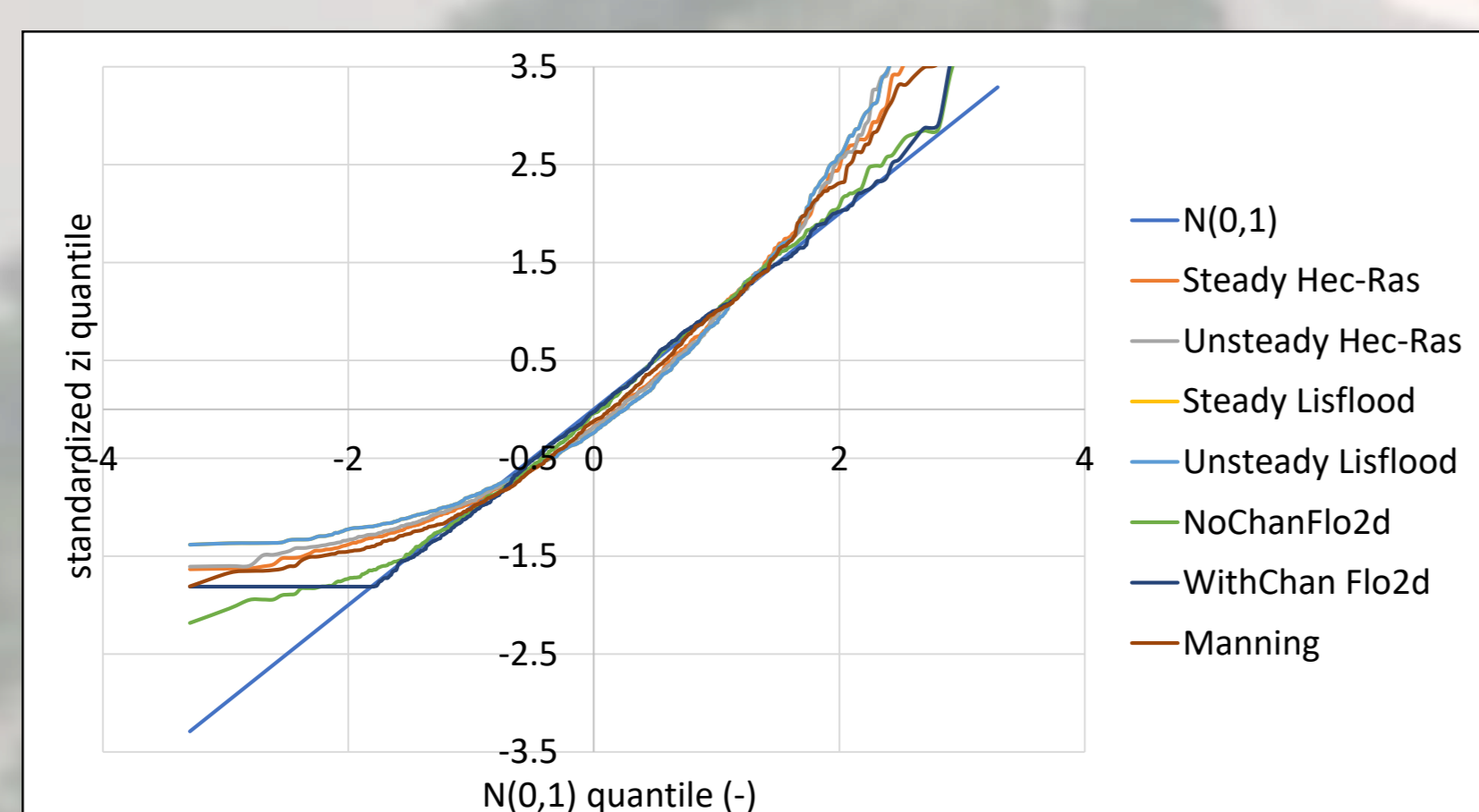


Figure 11: Q-Q plots of the water depth of the channels' upstream cell/section

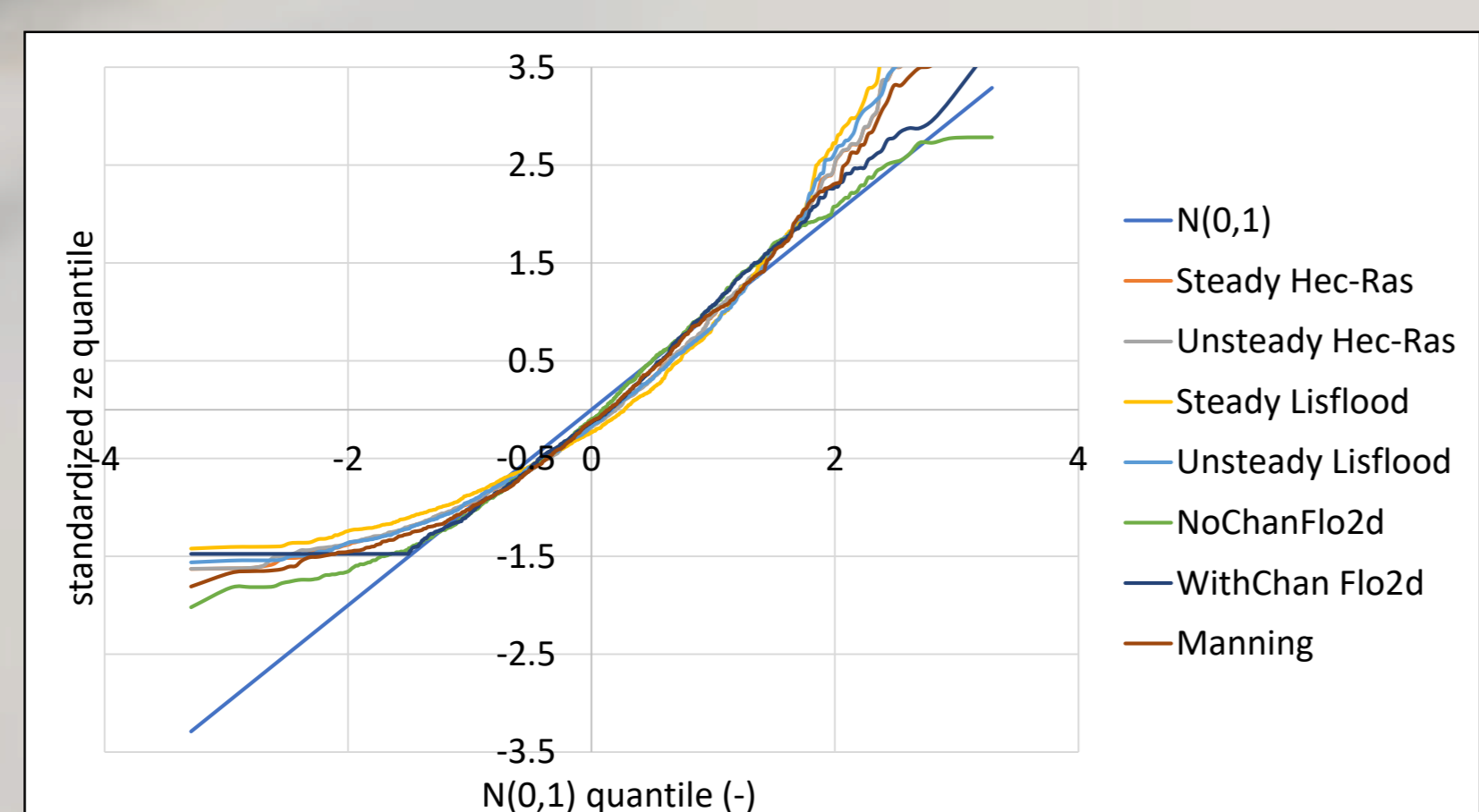


Figure 12: Q-Q plots of the water depth of the channels' downstream cell/section

4 Brief description of the hydraulic software tools

1. HEC-RAS

- 1D flood routing
- Implicit-forward finite difference scheme
- Sufficiently represent the topography (not raster-based)
- Low computational cost and powerful in 1D steady flow simulations
- The steady flow scheme is based on the 1D energy equation
- The unsteady flow scheme is based on the 1D Saint-Venant equations

2. FLO-2d

- Raster-based
- Allows flexible geometry of the channel and the floodplain terrain
- Solves the 1D Saint-Venant equations
- Explicit-central finite difference scheme
- Suitable for large grid cell size

3. LISFLOOD-FP

- Quasi-2d (channel and floodplain routings are within sensitivity analysis and associated range of feasible values; all variables are uniformly distributed, except for the model resolution determined by the channel width, which takes three discrete values with equal probability (50 or 100 m).
- Suitable for large basins with wide and shallow channels
- Assumes a rectangular channel section
- Backward-implicit numerical scheme
- For the flood routing is used the 1D kinematic wave (positively varying channel gradient) and the diffusive wave (negative channel gradient and lateral flow propagation)

4. SIMPLE MODEL WITH THE USE OF MANNING EQUATION

- Manning's equation is an empirical equation that applies uniform flow in open channels
- The bottom's slope is the same as the slope of the energy grade line and the water surface slope
- The equation is applied in the composite cross-section of the channel and the floodplain taking into account both roughness coefficients (channel's and floodplain's) with the use of Colebatch's equation.

5. Brief description and evaluation of the use and the results of OpenFOAM

- InterFoam (an OpenFOAM's solver for two-face flow)
- The VOF method used to solve the two-face flow with free surface (air-water)
- RANS (Reynolds Averaged Navier-Stokes) numerical scheme
- k-ε turbulence model
- The results of the Open FOAM for the water volume have high correlation with Steady Lisflood (correlation factor: 0.93) but the computational cost is a lot bigger

10 Variation coefficients of the flood volume vs. grouped input variables

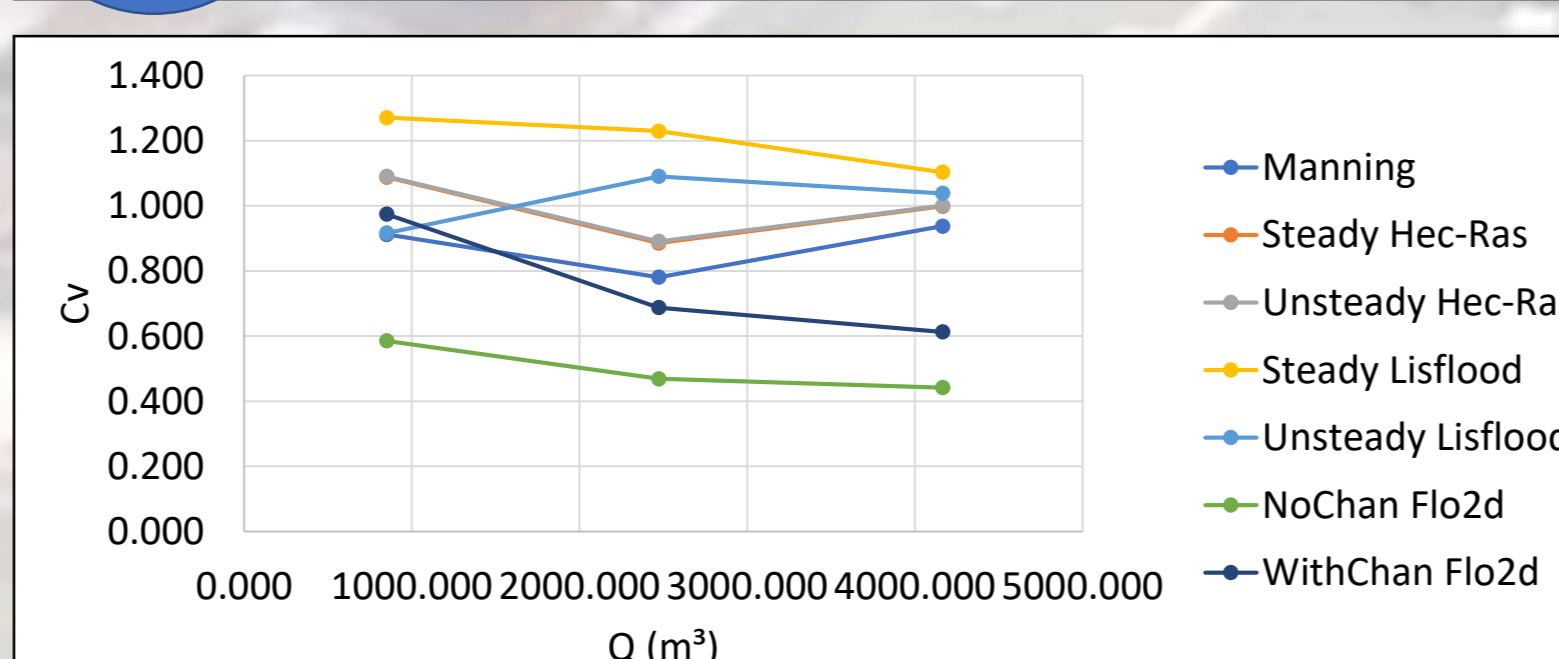


Figure 13: Variation coefficients of the flood volume vs. upstream flow

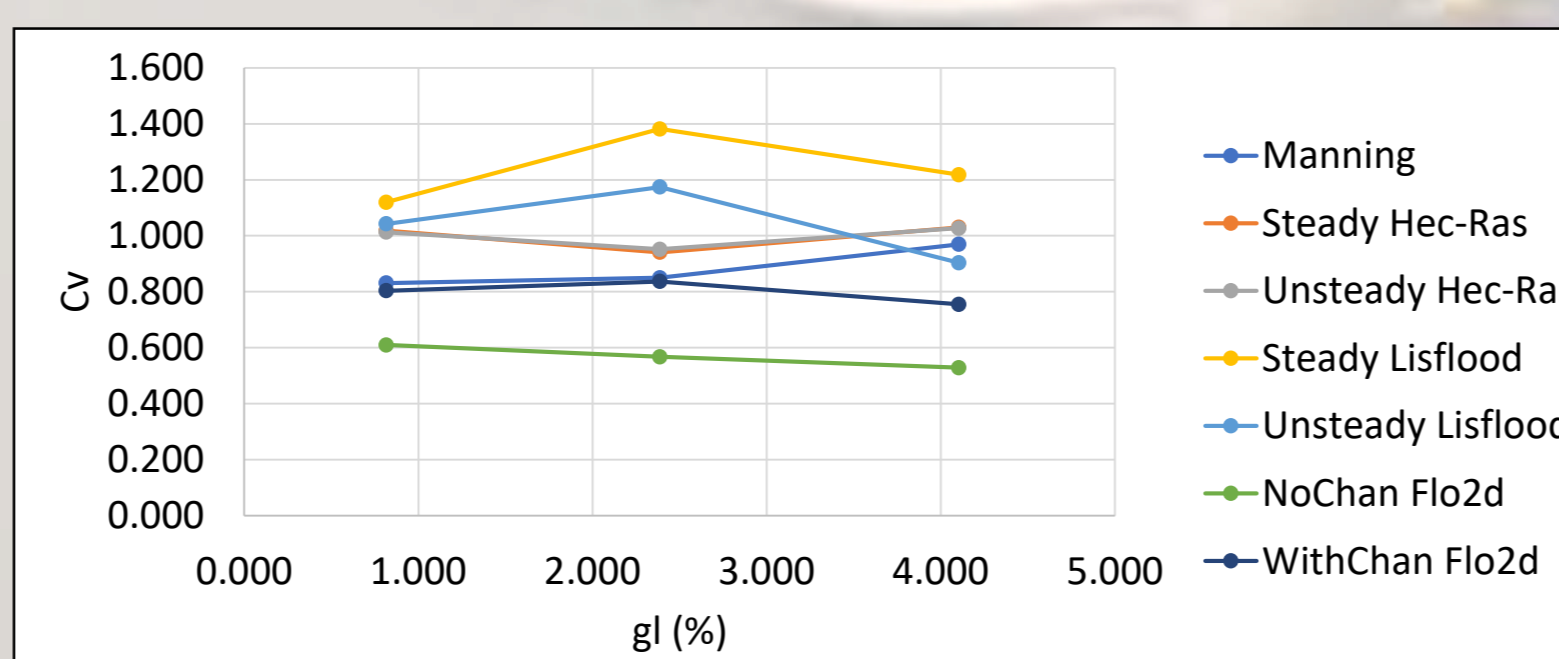


Figure 14: Variation coefficients of the flood volume vs. longitudinal gradient

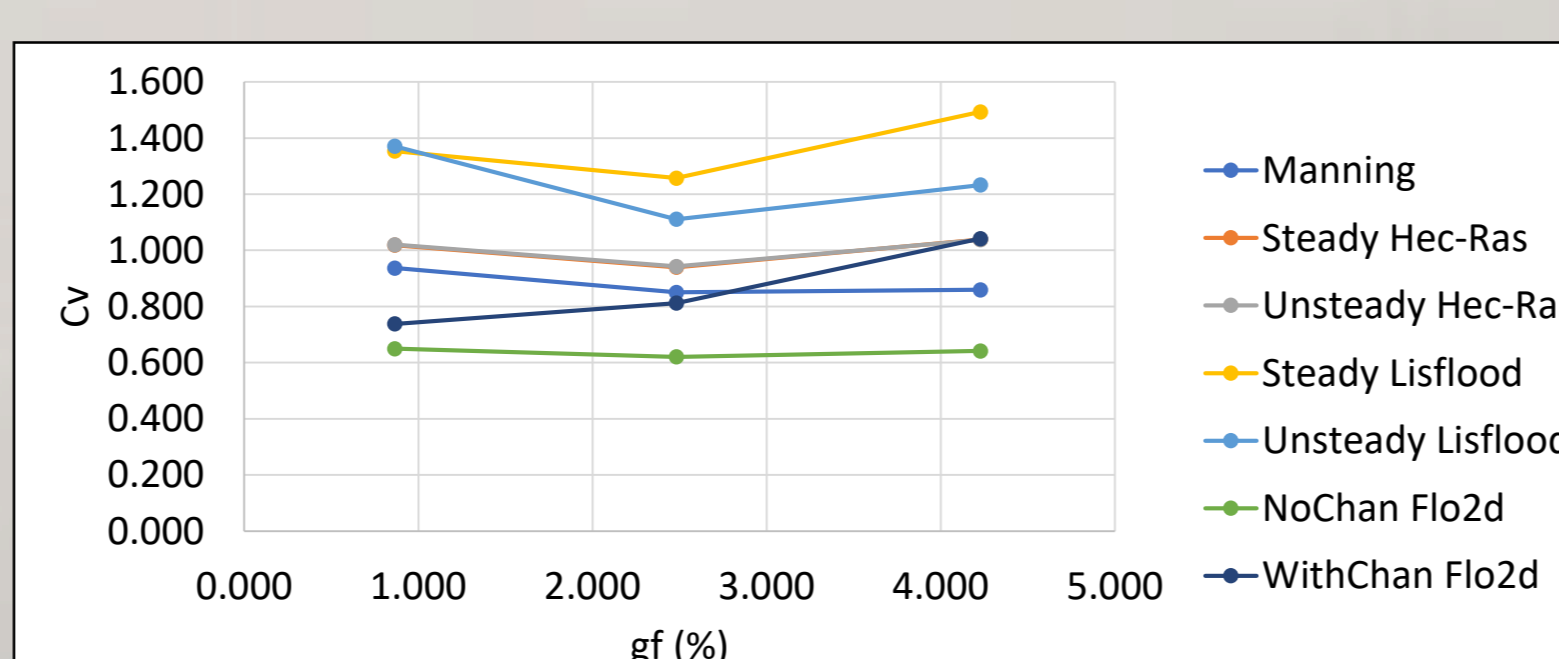


Figure 15: Variation coefficients of the flood volume vs. lateral gradient

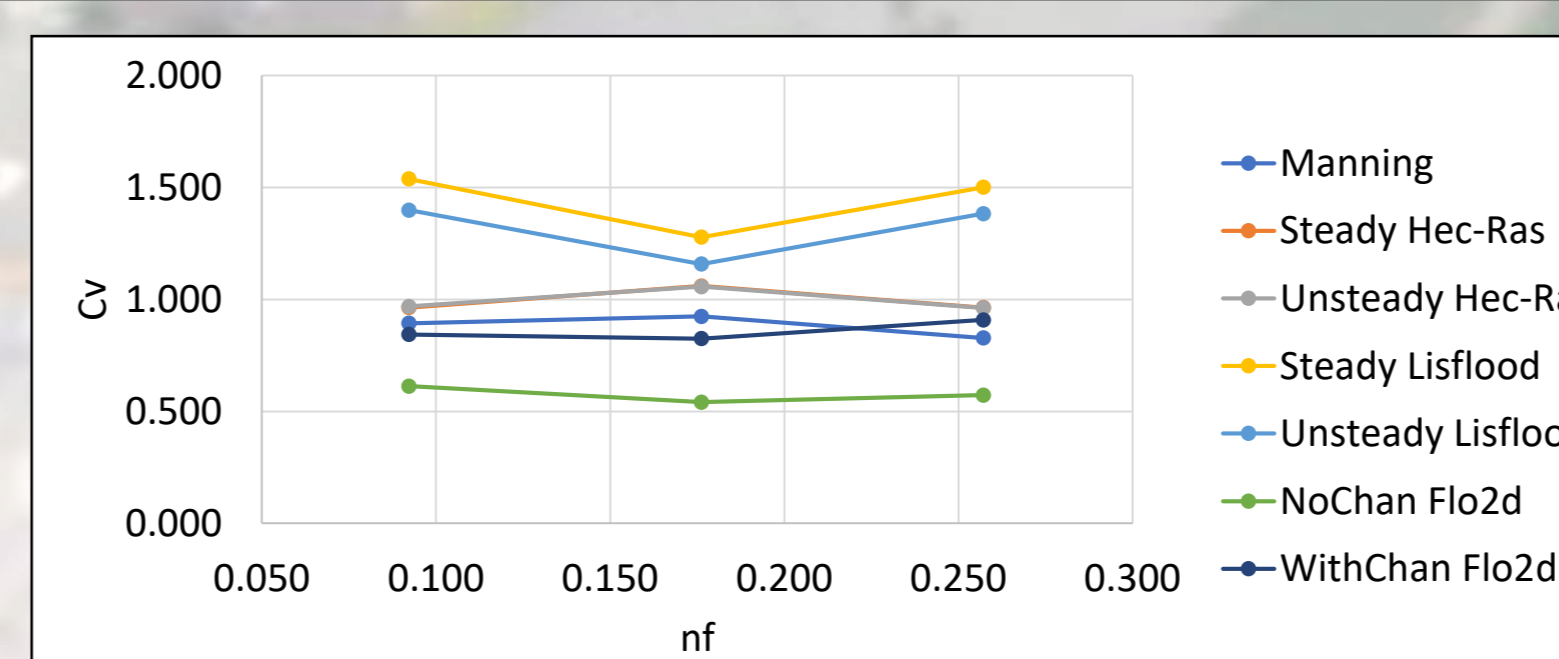


Figure 16: Variation coefficients of the flood volume vs. floodplain roughness coefficient

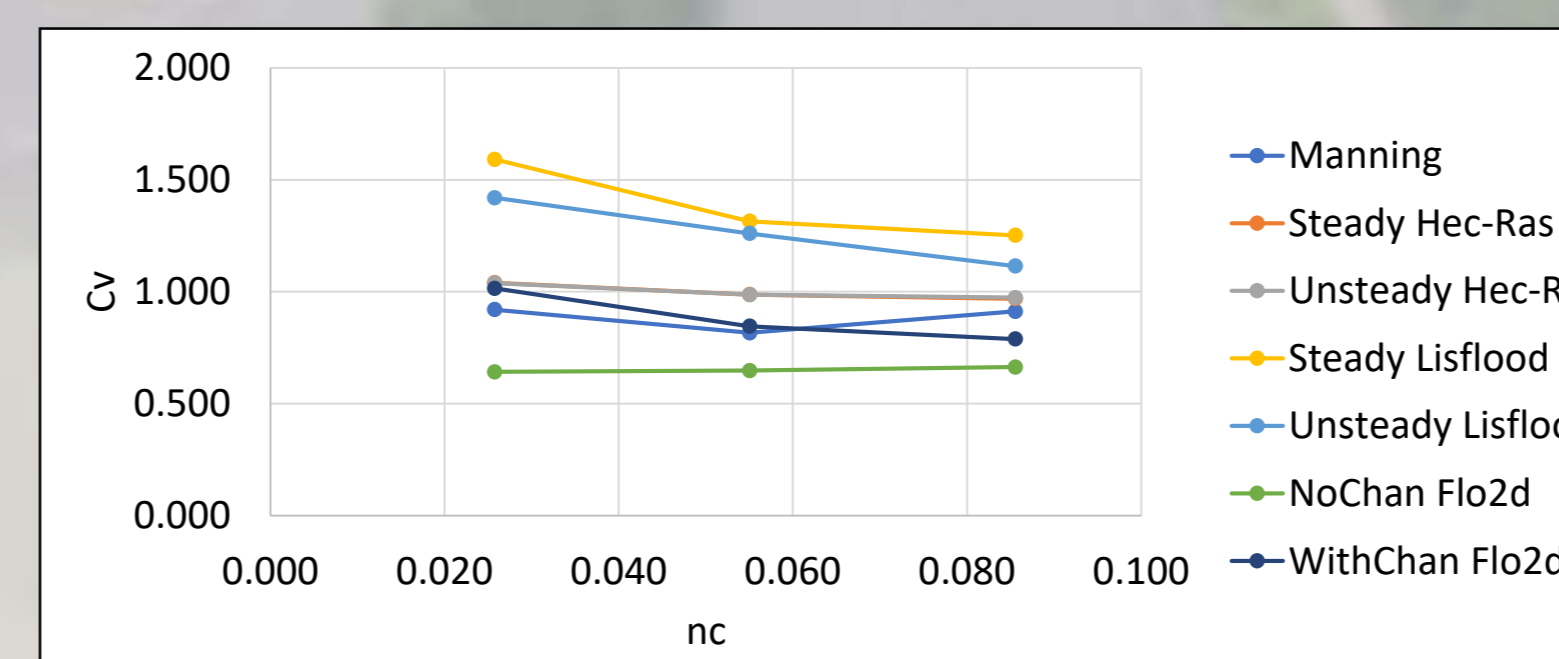


Figure 17: Variation coefficients of the flood volume vs. channel roughness coefficient

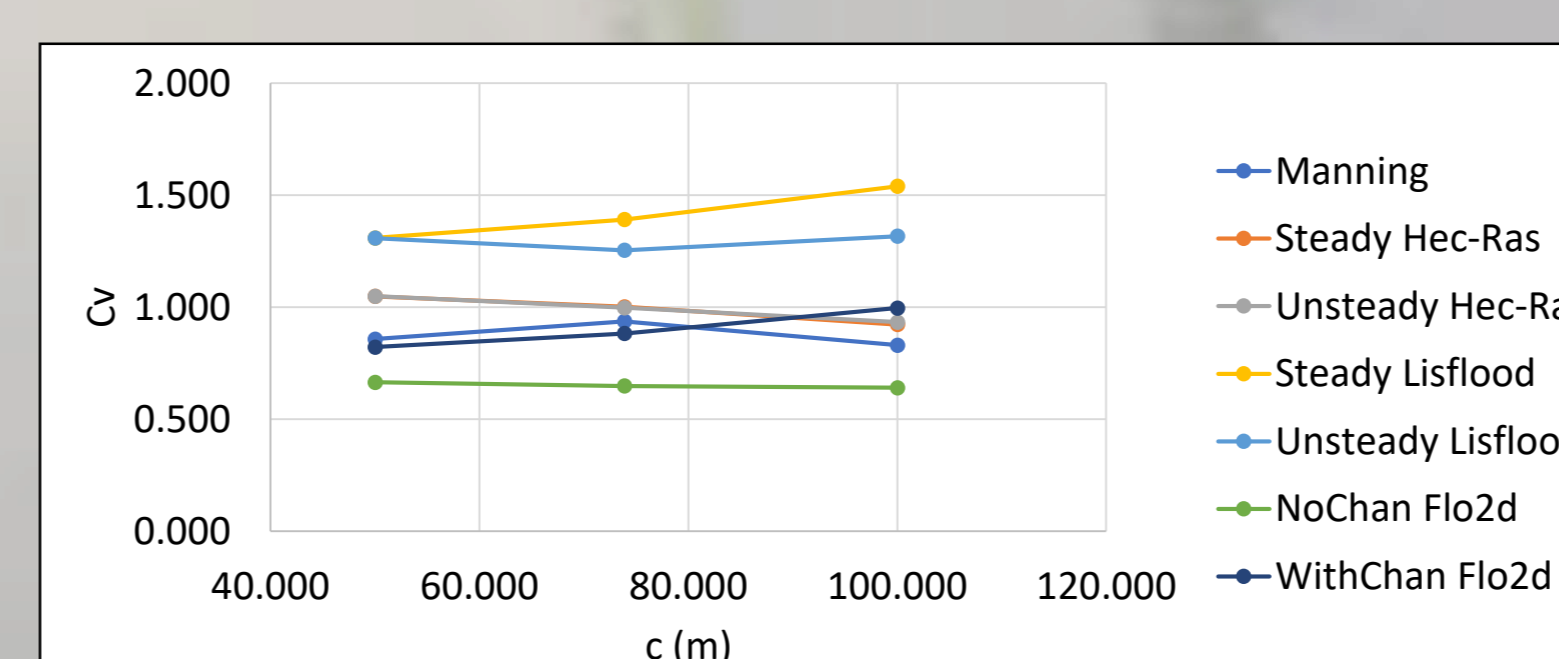


Figure 18: Variation coefficients of the flood volume vs. channel width

6 Moving average of coefficient of variation of the water depth of the channels' upstream and downstream cell/section

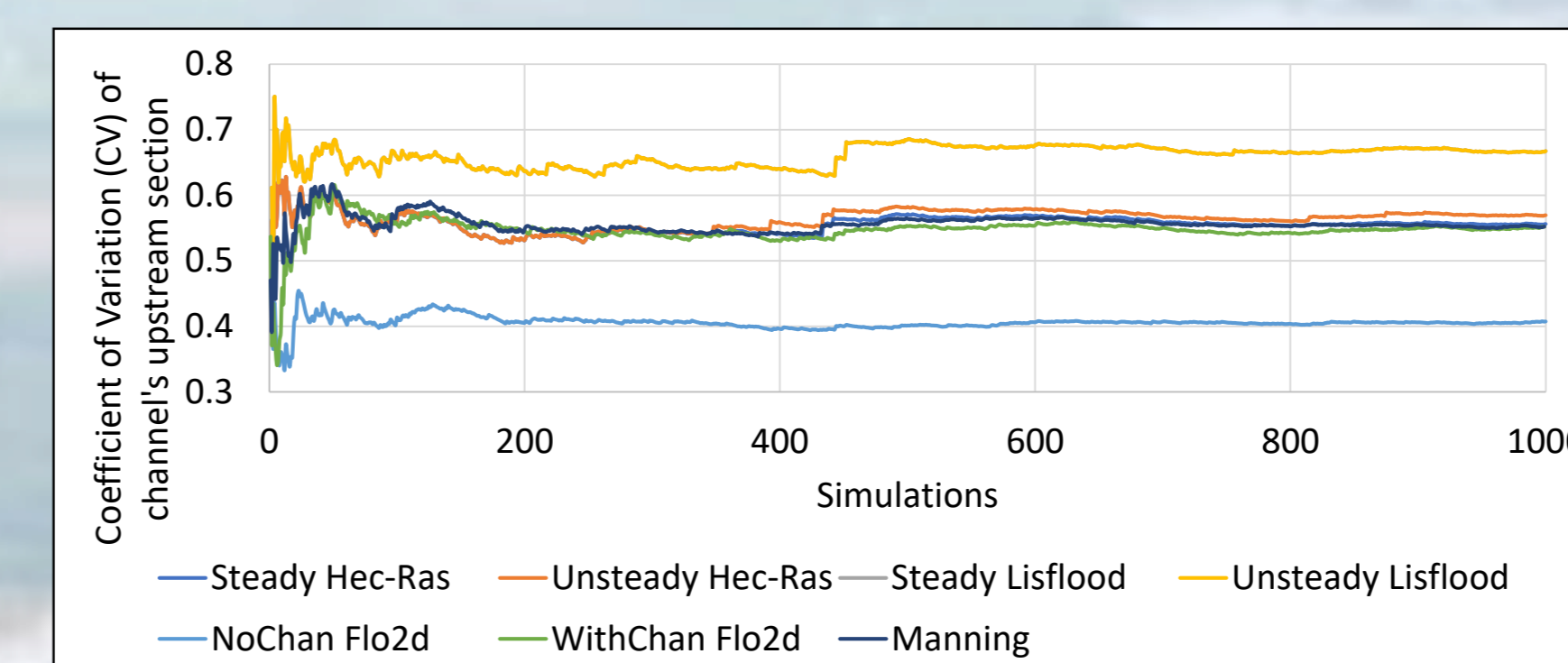


Figure 2: Moving average of coefficient of variation CV of the water depth of the channels' upstream cell/section

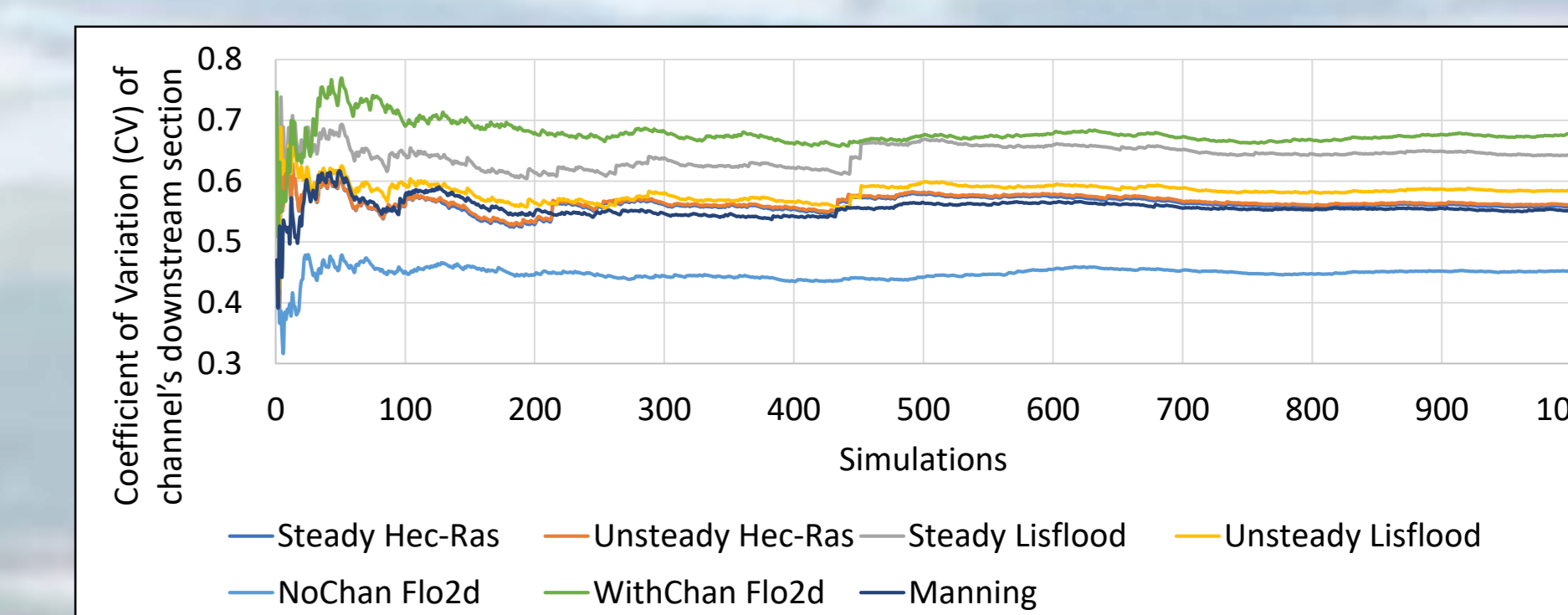


Figure 3: Moving average of coefficient of variation CV of the water depth of the channels' downstream cell/section

7 Moving average of mean, standard deviation and coefficient of variation for the flood volume

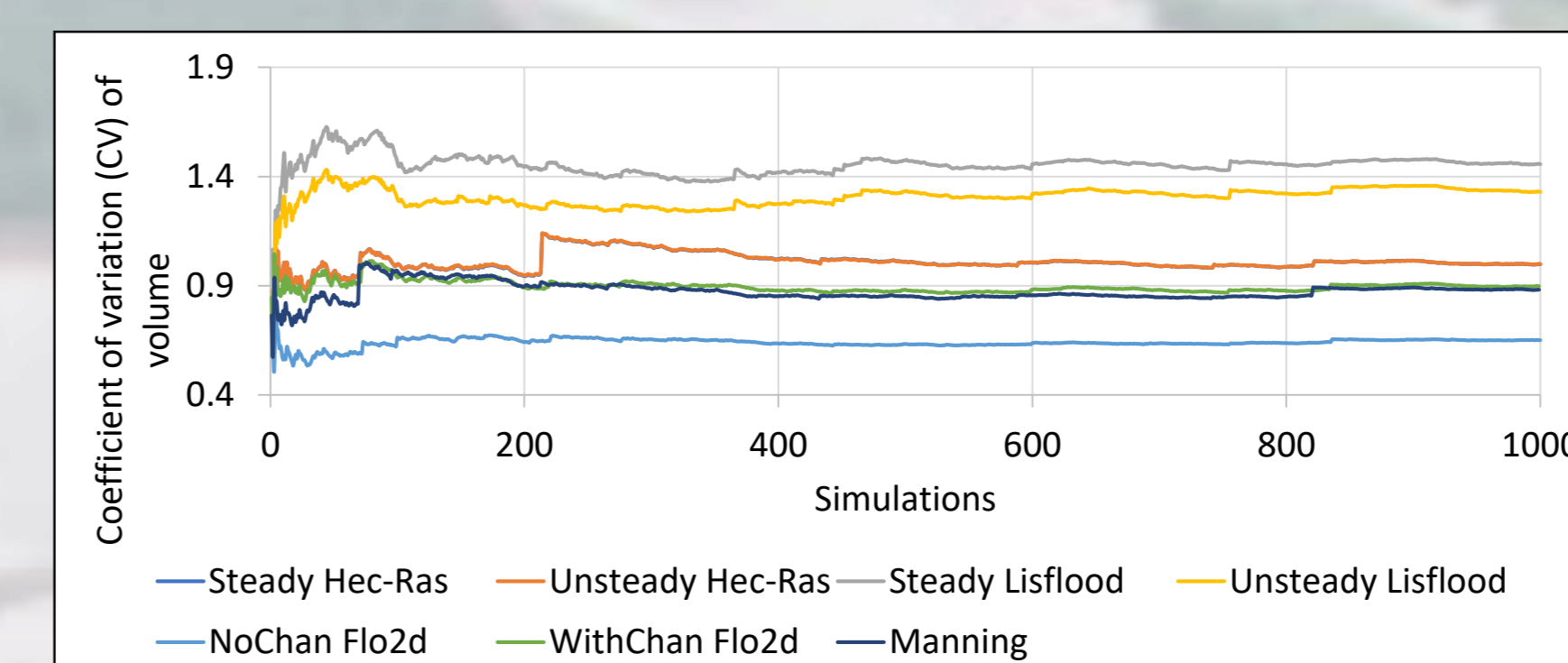


Figure 4: Moving average of the coefficient of variation for the flood volume

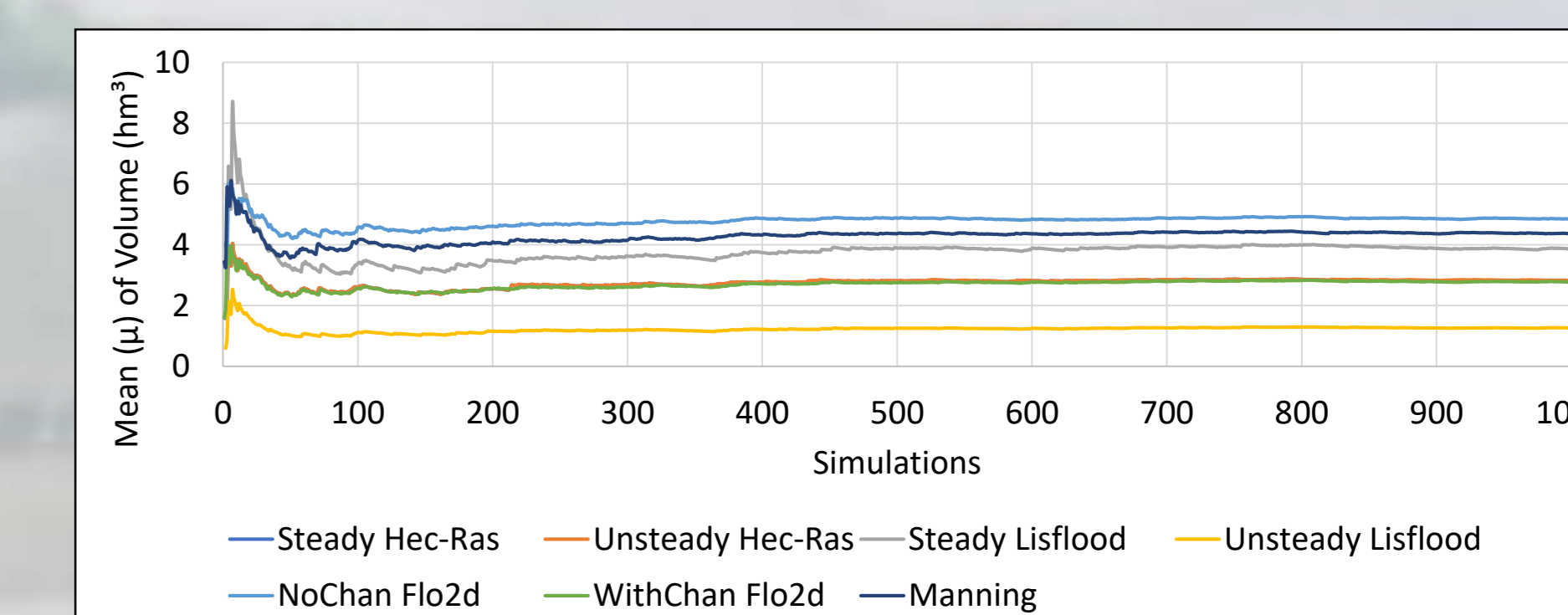


Figure 5: Moving average of mean for the flood volume

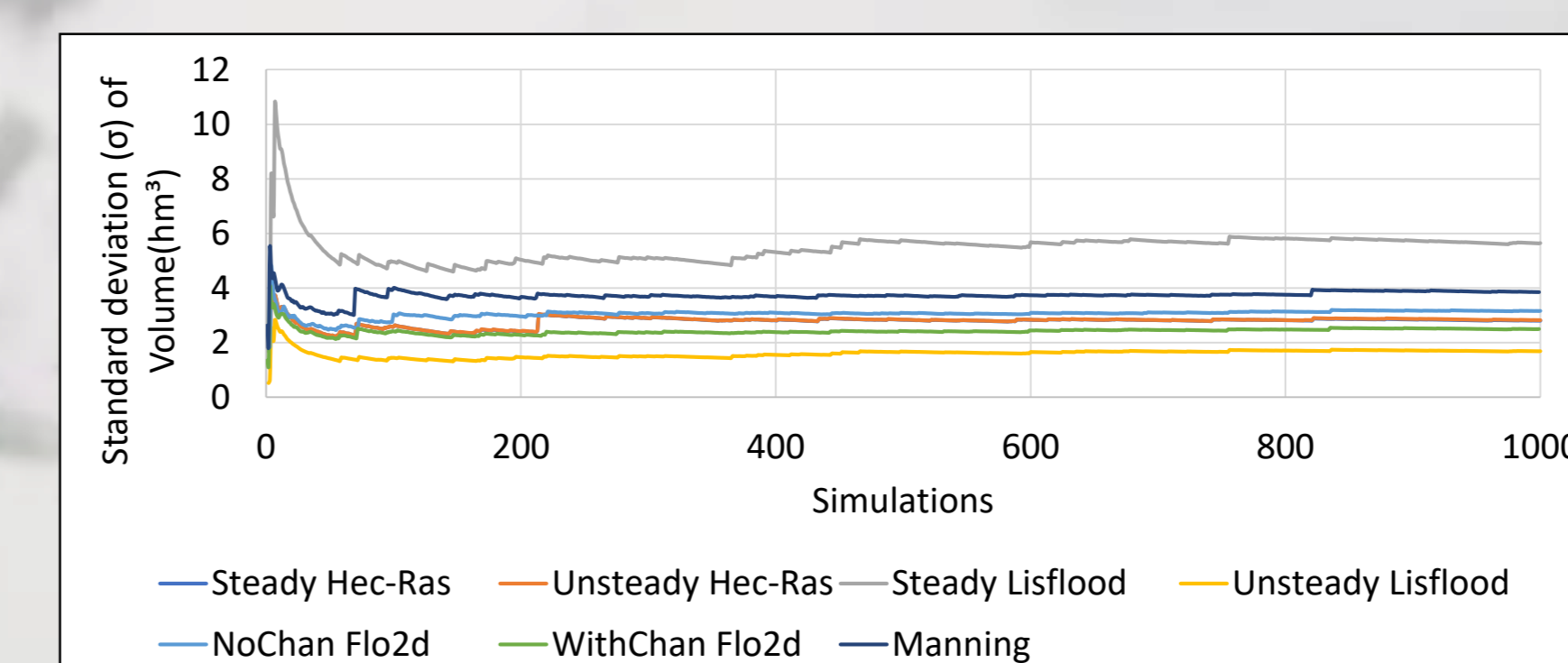


Figure 6: Moving average of standard deviation for the flood volume

11 Comparison of the models' results

	steady Hec-Ras	unsteady Hec-Ras	steady Lisflood	unsteady Lisflood	NoChan Flo2d	WithChan Flo2d	Manning
steady Hec-Ras	1.00	0.98	0.04	0.04	0.02	0.04	0.89
unsteady Hec-Ras	0.98	1.00	0.04	0.03	0.02	0.04	0.87
steady Lisflood	0.04	0.04	1.00	0.98	0.64	0.84	0.04
unsteady Lisflood	0.04	0.03	0.98	1.00	0.67	0.85	0.05
NoChan Flo2d	0.02	0.02	0.64	0.67	1.00	0.86	0.02
WithChan Flo2d	0.04	0.04	0.84	0.85	0.86	1.00	0.05
Manning	0.89	0.87	0.04	0.05	0.02	0.05	1.00

Table 2: Correlations of the flood volume between the models

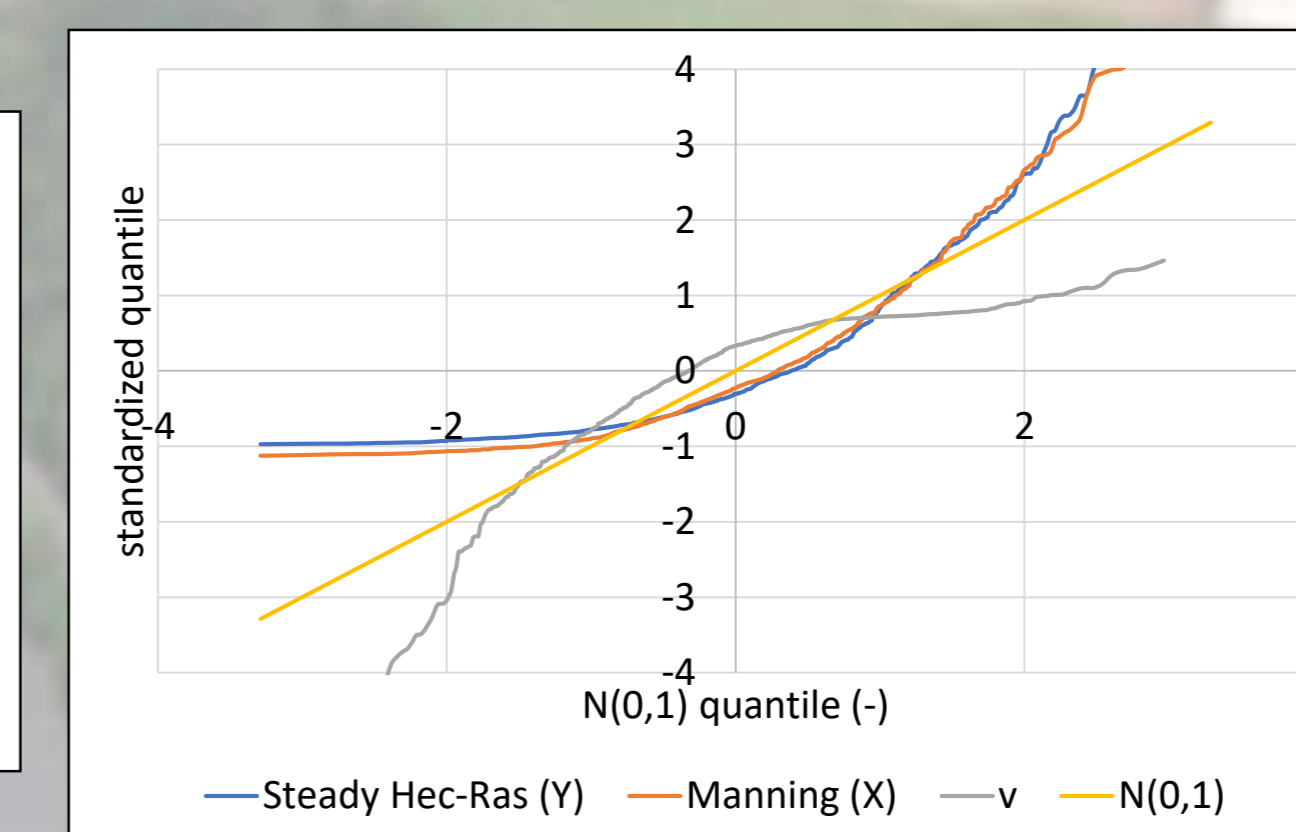


Figure 19: Q-Q plots of (Manning)X, (Hec-Ras)Y, V

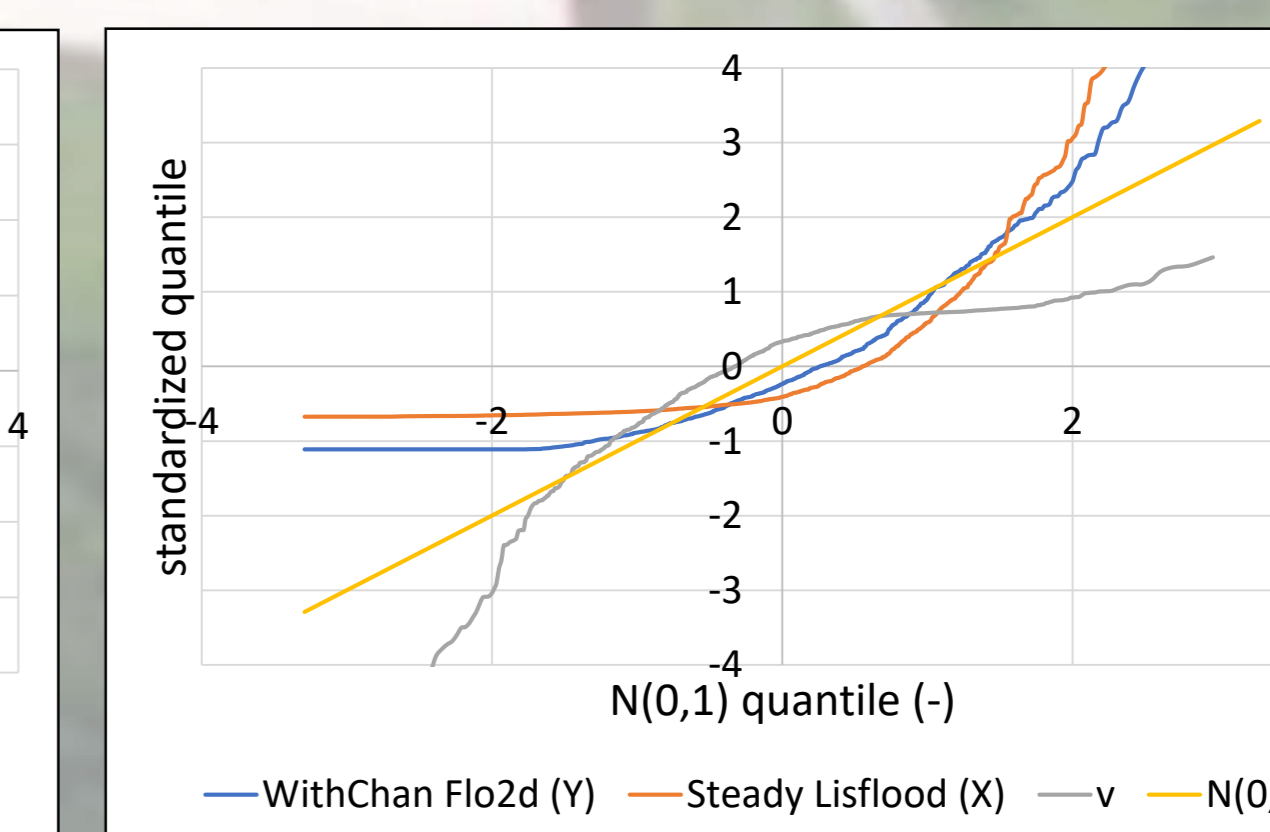


Figure 20: Q-Q plots of (Lisflood)X, (Flo2d)Y, V

12 Conclusions

- The empirical probability function of the flood volume follows heavy-right-tailed distributions (possible large uncertainty).
- The empirical probability function of the upstream and downstream water depths are close to normality.
- The empirical probability functions of the flood volume and the water depths (upstream and downstream) display positive skewness.
- The empirical probability function of the flood volume mainly follows well the lognormal distribution (MLE method was performed)
- The uncertainty in flood propagation stems from the channel and floodplain friction and the inflow discharge.
- The simple model that uses the Manning equation acts similarly to the other more complex models in terms of variability (uncertainty).

- The more simple Manning model is highly correlated with Hec-Ras, justified by their 1d nature.
- Furthermore, the other 1D/2D models seem to exhibit large correlation with the quasi-1D Steady Lisflood model.

- A linear stochastic model can be used to simulate the variability of more complex models (Y) through the more simple Manning or Lisflood model (X): $Y=PX+V$, where P is the correlation coefficient (the marginal distribution of V can be estimated if the distributions of X and Y are estimated from an extensive sensitivity analysis).

References

• Bellos, V., Kouritis, I., Moreno-Rodenas, A. and Tshirintzis, V., Quantifying Roughness Coefficient Uncertainty in Urban Flooding Simulations through a Simplified Methodology. *Water* 9(12), 944, 2017.

• Dimitriadis, P., A. Tegos, A. Oikonomou, V. Pagana, A. Koukouvintis, N. Mamassis, D. Koutsoyiannis, and A. Efstratiadis, Comparative evaluation of 1D and quasi-2D hydraulic models based on benchmark and real-world applications for uncertainty assessment in flood mapping, *Journal of Hydrology*, 534, 478–492, doi:10.1016/j.jhydrol.2016.01.020, 2016.

• Dimitriadis, P., A. Tegos, A. Petsiou, V. Pagana, I. Apostolopoulos, E. Vassilopoulos, M. Gini, A. D. Koussis, N. Mamassis, D. Koutsoyiannis, and P. Papanicolaou, Flood Directive implementation in Greece: Experiences and future improvements, 10th World Congress on Water Resources and Environment "Panta Rhei", Athens, European Water Resources Association, 2017.

• Domeneghetti, A., Vorogushyn, S., Castellari, A., Merz, B., Brath, A., Probabilistic flood hazard mapping: effects of uncertain boundary conditions. *Hydrology and Earth System Sciences*, 17: 3127–3140, 2013.

• Koutsoyiannis, D., Mamassis, N., Efstratiadis, A., Zarkadoulas, N., Markonis, Y., Floods in Greece. In: Kundzewicz, Z.W. (Ed.), *Changes of Flood Risk in Europe*. IAHS Press, International Association of Hydrological Sciences, Wallingford, pp. 238–256 (Chapter 12), 2012.

• Papaioannou, G., Loukas, A., Vasilades, L., Aronica, G.T., Flood inundation mapping sensitivity to riverine spatial resolution and modelling approach, *Natural Hazards*, 83(1):117–132, 2016.

• <https://www.hec.usace.army.mil/software/hecras/>

• <https://www.flo-2d.com/>

• <http://www.bristol.ac.uk/geography/research/hydrology/models/lisflood/>

• <https://openfoam.org/>